

METHODOLOGY

Open Access



A quadruple fluorescence quantitative PCR method for the identification of wild strains of african swine fever and gene-deficient strains

Xuezhi Zuo^{1,2†}, Guorui Peng^{1†}, Yingju Xia¹, Lu Xu¹, Qizu Zhao¹, Yuanyuan Zhu¹, Cheng Wang^{1,2}, Yebing Liu¹, Junjie Zhao¹, Haidong Wang^{1*} and Xingqi Zou^{2*}

Abstract

Background Originating in Africa, African swine fever (ASF) was introduced to China in 2018. This acute and highly virulent infectious disease affects domestic pigs. The World Organization for Animal Health has listed it as a statutory reportable disease, and China has listed it as a category A infectious disease.

Methods Primers and probes were designed for four ASFV genes (*B646L*, *EP402R*, *MGF505-3R*, and *A137R*). The primers/probes were highly conserved compared with the gene sequences of 21 ASFV strains.

Results After optimization, the calibration curve showed good linearity ($R^2 > 0.99$), the minimum concentration of positive plasmids that could be detected was 50 copies/ μL , and the minimum viral load detection limit was 10^2 $\text{HAD}_{50}/\text{mL}$. Furthermore, quadruple quantitative polymerase chain reaction (qPCR) with nucleic acids from three porcine-derived DNA viruses and cDNAs from eight RNA viruses did not show amplification curves, indicating that the method was specific. In addition, 1×10^6 , 1×10^5 , and 1×10^4 copies/ μL of mixed plasmids were used for the quadruple qPCR; the coefficient of variation for triplicate determination between groups was $< 2\%$, indicating the method was reproducible.

Conclusions The results obtained by testing clinical samples containing detectable *EP402R*, *MGF505-3R*, and *A137R* strains with different combinations of gene deletions were as expected. Therefore, the established quadruple qPCR method was validated for the molecular diagnosis of ASF using gene-deleted ASFV strains.

Keywords *A137R*, *B646L*, *EP402R*, African swine fever, Quadruple qPCR, *MGF505-3R*

[†]Xuezhi Zuo and Guorui Peng contributed equally to this work and share first authorship.

*Correspondence:

Haidong Wang
wanghaidong@sxau.edu.cn
Xingqi Zou
zouxingqi@163.com

¹College of Veterinary Medicine, Shanxi Agricultural University, Jinzhong 030801, Shanxi, China

²China/WOAH Reference Laboratory for Classical Swine Fever, China Institute of Veterinary Drug Control, Beijing, China



© The Author(s) 2023. **Open Access** This article is licensed under a Creative Commons Attribution 4.0 International License, which permits use, sharing, adaptation, distribution and reproduction in any medium or format, as long as you give appropriate credit to the original author(s) and the source, provide a link to the Creative Commons licence, and indicate if changes were made. The images or other third party material in this article are included in the article's Creative Commons licence, unless indicated otherwise in a credit line to the material. If material is not included in the article's Creative Commons licence and your intended use is not permitted by statutory regulation or exceeds the permitted use, you will need to obtain permission directly from the copyright holder. To view a copy of this licence, visit <http://creativecommons.org/licenses/by/4.0/>. The Creative Commons Public Domain Dedication waiver (<http://creativecommons.org/publicdomain/zero/1.0/>) applies to the data made available in this article, unless otherwise stated in a credit line to the data.

Introduction

African swine fever (ASF) is a highly contagious viral disease caused by the African swine fever virus (ASFV), a double-stranded DNA virus belonging to the *Asfarviridae* family, which has 24 known genotypes [1, 2]. Its genome ranges between 170 and 193 kbp in length and encodes 68 structural proteins and >100 non-structural proteins [3]. The virus comprises four layers of protein shells and an endogenous genome with a significantly more complex structure than many other viruses. In addition, its multilayered structure plays an important role in its replication and survival [4].

The p72 protein encoded by the B646L gene of ASFV is a major coat protein expressed at a late stage with a differential sequence in the C-terminal region [3]. Thus far, ASFV has been classified into 24 genotypes based on partial sequencing of the *B646L* gene encoding p72 [1, 2]. The main strains prevalent in China are genotypes II (reported in 2018) [5] and I (reported in 2021) [6]. In addition, the *EP402R* gene encodes a late expressed CD2v protein, a glycoprotein similar to the surface adhesion receptor CD2v on T lymphocytes [7]. Viral CD2v protein is involved in the adsorption of erythrocytes, the binding of extracellular virus particles to erythrocytes [7], host immune regulation, virulence, and induction of protective immune responses [8]. Multigene family (MGF) proteins are widely distributed in ASFV and are generally classified into five families: MGF-100, MGF-110, MGF-300, MGF-360, and MGF-505 [9]. MGF proteins are reported to be early expressed proteins [10] and are key players in multiple stages of transcription, translation, virulence, and immune escape in virally infected host cells [11]. The A137R protein is expressed late during the viral replication cycle, inhibits the interferon signaling pathway, and plays an important role in evading the innate immune response [12]. In the artificial construction of gene-deleted strains, genes such as *EP402R*, *MGF*,

and *A137R* are usually targeted; therefore, establishing corresponding detection methods is necessary for clinical applications.

The diagnosis of ASFV involves a virus isolation–erythrocyte adsorption assay (HAD), polymerase chain reaction (PCR), real-time fluorescent quantitative PCR (qPCR), and isothermal amplification techniques. Virus isolation is a confirmatory method, and its corresponding assay (the erythrocyte adsorption assay) is time-consuming and can be used only to validate strains with erythrocyte adsorption characteristics. Moreover, it must be conducted in a biosafety level III laboratory to measure viral activity in samples and is dependent on the presence of actively replicating virus, which may be absent if the sample has not been correctly stored, resulting in inactivation, thus limiting its clinical applications [13]. The isothermal amplification technique is suitable for rapid on-site detection. However, its sensitivity is slightly less than that of fluorescent PCR. Furthermore, although the PCR method has good specificity, its sensitivity is relatively low, the procedure is cumbersome, and aerosol contamination can easily occur, limiting its applications [14]. However, fluorescent PCR, which has high sensitivity, good specificity, and a convenient procedure, is gradually becoming the main method for ASFV diagnosis. In this technique, the highly sensitive qPCR is the standard method [15].

Because using multiple methods and experiments to detect multiple genes is time-consuming and laborious, only a few genes have been detected using the currently available qPCR methods. In this study, we designed primers/probes for four ASFV genes (*B646L*, *EP402R*, *MGF505-3R*, and *A137R*) and established a quadruple fluorescent qPCR assay to diagnose ASF and differentiate gene-deleted strains from wild-type strains.

Materials and methods

Design of primers and probes

Primers/probes for amplifying *B646L*, *EP402R*, *A137R*, and *MGF505-3R* were designed using Primer3 (<https://primer3.org/>) and were subjected to BLAST analysis. The primers/probes were compared with several ASFV strains published in GenBank using SnapGene software (www.snapgene.com/). The primers/probes (Table 1) were all synthesized by Sangon Biotech (Shanghai, China). The sequences and sizes of the target fragments amplified by the designed primer probes in the Georgia 2007/1 strain are shown in Supplementary file 1, Figs. 1, 2, 3 and 4.

Plasmid construction and nucleic acid extraction

With reference to the ASFV HuB20 strain (GenBank sequence number: MW521382), full-length *B646L*, *EP402R*, *A137R*, and *MGF505-3R* genes were

Table 1 Primer/probe sequences

Target gene	Primer/probe	Sequences (5'–3')
<i>B646L</i>	B646L-F	GAACGTGAACCTTGCTA
	B646L-R	GGAAATTCATTCACCAAATCC
	B646L-P	6-FAM -TAAAGCTTGTCATCGCA- MGB
<i>EP402R</i>	EP402R-F	GACACCACTTCATACATGAAC
	EP402R-R	GGACGCATGTAGTAAATAGGT
	EP402R-P	Cy5 -CAGTCGTTATCAGTATAA- MGB
<i>A137R</i>	A137R-F	CTTGAATCCCTGAGGAACG
	A137R-R	CGATGTCCCAGAAATGAGTCT
	A137R-P	Texas Red -CACCGCCTGGCATGA- MGB
<i>MGF505-3R</i>	MGF505-3R-F	GAGCTGTTGTTGTCATGGGA
	MGF505-3R-R	GGATTTTGAATCAGCGGCAA
	MGF505-3R-P	VIC -CCCCGCTACGCCGTCGTAG- GAGCCC- MGB

(A)



(B)



(C)



(D)



Fig. 1 (A–D) The primers/probes of *B646L*(A), *EP402R*(B), *A137R*(C), and *MGF505-3R*(D) with the gene sequence comparison of African swine fever virus (ASFV) endemic strains in China and other countries. The red boxes correspond to the sequence for upstream primers, the blue boxes to the sequence for probes, and the black boxes to the sequence for downstream primers

synthesized, ligated into the pUC57 vector, and used as a positive control. The recombinant plasmids were named pUC57-B646L, pUC57-EP402R, pUC57-A137R, and pUC57-MGF505-3R; their concentrations were converted to copy numbers after measuring their OD₂₆₀ using a Nanodrop-1000 microspectrophotometer (Thermo Fisher Scientific; Waltham, MA, USA). The four recombinant plasmids were mixed so that the concentration of each recombinant plasmid was 2.5×10^8 copies/ μL . Next, the mixed plasmids were diluted to 1×10^8 copies/ μL , and 10-fold dilutions were performed to obtain 1×10^0 copies/ μL ; 1×10^2 copies/ μL of the mixed plasmids was twice diluted in half to obtain 25 copies/ μL . Lastly, clinical and diluted samples from the 10^8 – 10^0 HAD₅₀ ASFV blood series were subjected to nucleic acid extraction using the QIAamp DNA Mini Kit (Cat No. 51,306; Qiagen, Hilden, Germany).

Quadruple fluorescence quantitative PCR method optimization

Using a LightCycler 480II fluorescent qPCR instrument (Roche Holding AG, Basel, Switzerland), 2 \times HyperProbe Mixture (CW BIO, Cat No. CW3003M, Beijing, China) was selected as the premix required for the reaction, and the primer/probe concentration, annealing temperature, and cycle number were optimized. Next, the total system (Table 2) was optimized to 25 μL . Predenaturation at 95 °C for 30 s, denaturation at 95 °C for 10 s, and annealing/extension at 58 °C for 20 s were the qPCR reaction conditions. Because of interference between the fluorescence channels, the color compensation procedure was 95 °C for 30 s, 65 °C for 1 min, and 85 °C continuous.

Table 2 Quadruple quantitative polymerase chain reaction mixture components

Reagents	Volume (μL)
2 \times HyperProbe Mixture	12.5
B646L-F (20 μM)	0.3
B646L-R (20 μM)	0.3
B646L-P (10 μM)	0.2
EP402R-F (20 μM)	0.2
EP402R-R (20 μM)	0.2
EP402R-P (10 μM)	0.4
A137R-F (10 μM)	0.4
A137R-R (10 μM)	0.4
A137R-P (10 μM)	0.6
MGF505-3R-F (10 μM)	0.2
MGF505-3R-R (10 μM)	0.2
MGF505-3R-P (10 μM)	0.1
DNA	3
ddH ₂ O	6
Total	25

ddH₂O, double-distilled water

Establishment of a standard curve

A 10-fold serial dilution of 1×10^6 copies/ μL of the mixed plasmid to 10^2 copies/ μL was used as a template for quadruple qPCR amplification. Based on the cycle threshold (Ct) and copy number of the template, a standard curve was generated, and its slope and coefficient of determination (R^2) were determined.

Sensitivity

Mixed plasmids of 1×10^3 , 1×10^2 , 50, 25, and 1 copies/ μL were used as reaction templates to test the sensitivity of the quadruple qPCR. In brief, blood samples with a viral load of 10^8 HAD₅₀ ASFV were diluted 10-fold to 10^0 HAD₅₀, and nucleic acids were extracted to test the sensitivity of quadruple qPCR for detecting nucleic acid templates representing different viral loads.

Specificity and reproducibility

The specificity of the quadruple qPCR was determined using nucleic acids of foot and mouth disease virus (FMDV), bovine viral diarrhea virus (BVDV), porcine epidemic diarrhea virus (PEDV), pseudorabies virus (PRV), porcine parvovirus (PPV), porcine reproductive and respiratory syndrome virus (PRRSV), swine influenza virus (SIV), porcine circovirus II (PCV2), Japanese encephalitis virus (JEV), classical swine fever virus (CSFV), transmissible gastroenteritis virus (TGEV), and ASFV kept in the WOA reference laboratory of the China Veterinary Drug Inspection Institute. In addition, 1×10^6 to 1×10^4 copies/ μL of mixed plasmids were used as templates for triplicate determinations, performed within and between groups of mixed plasmids of each gradient, to test the reproducibility of the quadruple qPCR. The standard deviation and coefficient of variation were calculated.

Clinical sample testing

The clinical samples collected included blood, liver, spleen, Hubei/2019 genotype II ASFV lung, Genotype 1 ASFV cell samples, and Artificial construction ASFV $\Delta\text{A137R}\Delta\text{EP402R}$ cell sample. Nucleic acids were extracted from these six samples (200 μL each) and were eluted with 50 μL of eluent, of which 3 μL each was used for the quadruple qPCR. The total system, with each primer/probe, ddH₂O, and 2 \times HyperProbe Mixture is presented in Table 2. The reaction conditions are described in Sect. 2.3.

Declarations

All treatments for viruses were performed in a Biosafety Level III Laboratory of the China Veterinary Drug Inspection Institute.

Results

Primer probe design

The gene sequence comparison of the prevalent ASFV strains in China and other countries revealed that the designed primers/probes matched conserved regions in *B646L*, *EP402R*, and *A137R* of ASFV genotypes I and II. In addition, the *MGF505-3R* primers/probes were conserved in genotype I Benin 97/1 (AM712239), genotype I OURT 88/3 (NC_044957), HeN/ZZ-P1/2021 (MZ945536), and SD/DY-I/2021 (MZ945537), and in genotype II strain L60 (KM262844) (Fig. 1 and Supplementary file 2). Therefore, we inferred that the *B646L* primer/probe could be used to confirm ASFV, after which the primers/probes of *EP402R*, *A137R*, and *MGF505-3R* were used to distinguish between the wild-type and gene-deleted ASFV strains.

Standard curves

The standard curves obtained using 1×10^6 to 1×10^2 copies/ μL of mixed plasmids as templates demonstrated good linearity. Moreover, the slopes of the standard curve equations for *B646L*, *EP402R*, *A137R*, and *MGF505-3R* were -3.737 , -3.707 , -3.832 , and -4.316 , respectively; the coefficients of determination (R^2) were 0.9962, 0.9970, 0.9940, and 0.9922, respectively (Fig. 2 and Supplementary file 3 Figs. 1, 2, 3 and 4). This data indicates that the

amplification efficiency of the method was good, and the fit was excellent.

Minimum detection limit and result determination

Among the mixed plasmids of 1×10^3 , 1×10^2 , 50×10^1 , 25×10^1 , and 1×10^1 copies/ μL , the minimum limit of detection was 50×10^1 copies/ μL for *B646L*, *EP402R*, *A137R*, and *MGF505-3R*, while their C_t values were 39.22, 39.19, 39.76, and 37.30, respectively (Table 3). Furthermore, the minimum limit of detection of 10^2 HAD₅₀/mL was determined using a 10-fold serial dilution of 10^8 HAD₅₀ ASFV blood samples. The C_t values of *B646L*, *EP402R*, *A137R*, and *MGF505-3R* in 10^2 HAD₅₀ nucleic acids were 39.62, 37.93, 38.13, and 35.92, respectively (Table 4).

The criteria for determining negative and positive results were based on the results for known low viral load, low copy-number positive plasmid samples, and sensitivity. For *B646L*, a $C_t \leq 37$ was considered positive, and $C_t > 40$ was considered negative. For *EP402R*, a $C_t \leq 38$ was considered positive, and $C_t > 40$ was considered negative. For *A137R*, a $C_t \leq 37$ was considered positive, and $C_t > 40$ was considered negative. For *MGF505-3R*, a $C_t \leq 36$ was considered positive, and $C_t > 38$ was considered negative. For each gene, no C_t value was considered

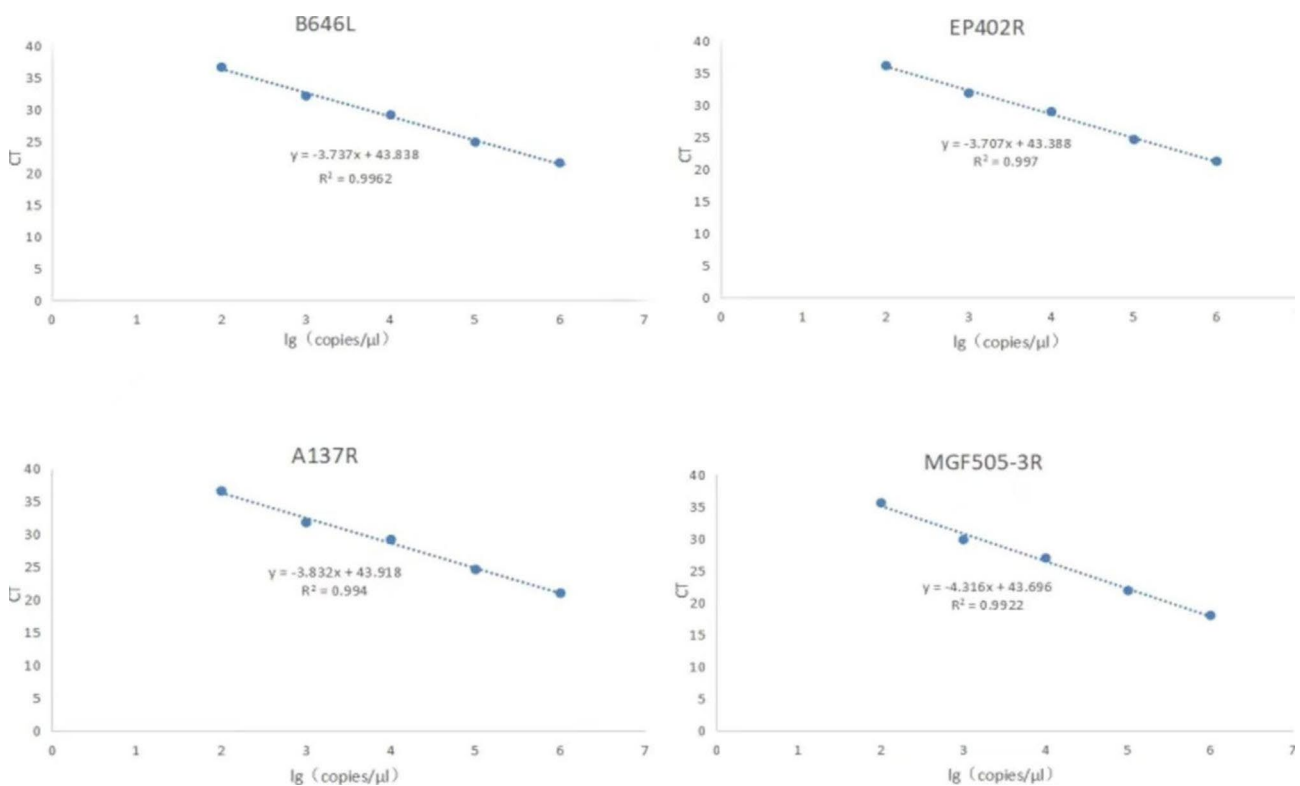


Fig. 2 Plot of standard curve equations for *B646L*, *EP402R*, *A137R*, and *MGF505-3R* genes in the quadruple quantitative polymerase chain reaction. *B646L*: $y = -3.737x + 43.838$, $R^2 = 0.9962$. *EP402R*: $y = -3.707 + 43.388$, $R^2 = 0.997$. *A137R*: $y = -3.832x + 43.918$, $R^2 = 0.994$. *MGF505-3R*: $y = -4.316x + 43.696$, $R^2 = 0.9922$

Table 3 Cycle threshold values of plasmids with different copy numbers for each gene

	<i>B646L</i>			<i>EP402R</i>			<i>A137R</i>			<i>MGF505-3R</i>		
	Repeat	Mean	SD	Repeat	Mean	SD	Repeat	Mean	SD	Repeat	Mean	SD
1×10^3 copies/ μ L	32.55	32.51	0.12	33.59	33.10	0.42	33.98	33.63	0.33	30.53	30.35	0.37
	32.38			32.86			33.60			30.60		
	32.60			32.85			33.32			29.92		
1×10^2 copies/ μ L	37.34	37.03	0.27	38.34	38.35	0.22	37.69	37.61	0.33	36.73	36.13	0.78
	36.93			38.14			37.89			36.41		
	36.83			38.58			37.25			35.25		
50 copies/ μ L	39.55	39.22	0.30	38.42	39.19	0.67	39.90	39.76	0.40	36.97	37.30	0.60
	39.15			39.51			39.31			36.94		
	38.95			39.64			40.09			38.00		

25 copies/ μ L

SD, standard deviation.

negative, and values between the positive and negative cut-offs were considered suspicious.

Specificity and reproducibility of the experimental results

DNA (PRV, PPV, and PCVII) and RNA viruses (FMDV, CSFV, PEDV, TGEV, SIV, JEV, PRRSV, and BVDV) did not show amplification curves in the quadruple qPCR; only the positive control for ASFV showed typical amplification (Fig. 3), indicating that the established method had good specificity.

The 1×10^6 to 1×10^4 copies/ μ L of mixed plasmids showed good reproducibility in the three replicates between groups within the quadruple qPCR, with coefficients of variation of less than 2% in all cases (Table 5).

Quadruple qPCR method validation

The clinical samples tested using the established quadruple qPCR showed the expected amplification. ASFV nucleic acids from the blood, liver, spleen, and lungs showed amplification; however, the *MGF505-3R* of genotype I ASFV and the *A137R* and *EP402R* of ASFV Δ A137R Δ EP402R did not show amplification (Fig. 4).

Discussion

Since its discovery, the continuous spread of ASF has significantly affected the global supply of pork products and has devastated food security and animal health and welfare [16]. China's pig production capacity has decreased significantly since the disease was introduced in 2018. Because of the insidiousness and complexity of ASFV transmission, the epidemic remains unresolved [17]. Although ASF has long been identified, it lacks a safe and effective vaccine. Therefore, an effective diagnostic method is critical for controlling the epidemic. Consequently, we designed primers/probes for four genes, *B646L*, *EP402R*, *A137R*, and *MGF505-3R*. Notably, the p72 protein, the main capsid protein of ASFV encoded by the *B646L* gene, is often used as the first choice for diagnosing epidemic ASFV [18–21]. In addition, CD2v, encoded by the *EP402R* gene, is vital for ASFV diagnosis [22, 23]. Furthermore, *EP402R*, *MGF*, and *A137R* are known virulence genes whose deletion can substantially reduce the virulence of the virus in pigs [23–30]. Therefore, these genes are expected to serve as alternative deletion genes for gene deletion vaccines, and establishing corresponding identification methods is necessary. Moreover, mutant strains such as CD2v-deletion strains with low pathogenicity have previously been identified [31]. We considered that targeting these ASFV genes would be necessary to confirm the diagnosis and pathogenic strains involved in ASFV infection. Thus, we developed a suitable quadruple PCR method that showed high sensitivity and specificity.

Table 4 Cycle threshold values of nucleic acids with different viral loads for each gene

	B646L			EP402R			A137R			MGF505-3R		
	Repeat	Mean	SD	Repeat	Mean	SD	Repeat	Mean	SD	Repeat	Mean	SD
10 ⁷ HAD ₅₀	22.90	22.77	0.27	22.95	22.83	0.19	21.80	21.61	0.28	18.48	18.09	0.35
	22.46			22.62			21.28			17.98		
10 ⁶ HAD ₅₀	22.95	25.59	0.06	22.94	25.50	0.21	21.74	24.43	0.30	17.80	21.41	0.27
	25.60			25.47			24.42			21.23		
	25.53			25.31			24.13			21.26		
10 ⁵ HAD ₅₀	25.64	28.62	0.09	25.72	28.73	0.10	24.73	27.82	0.12	21.72	25.05	0.20
	28.72			28.65			27.74			24.90		
	28.54			28.69			27.77			24.96		
10 ⁴ HAD ₅₀	28.59	31.89	0.18	28.84	32.15	0.24	27.95	31.27	0.41	25.28	28.49	0.52
	31.93			32.01			31.44			27.90		
	31.70			32.01			30.80			28.78		
10 ³ HAD ₅₀	32.05	35.17	0.47	32.43	34.87	0.49	31.57	34.25	0.49	28.79	32.18	0.26
	35.71			34.40			34.73			32.32		
	34.90			34.82			33.75			31.89		
10 ² HAD ₅₀	34.89	39.62	1.27	35.39	37.93	0.47	34.28	38.13	1.12	32.35	35.92	2.34
	41.07			37.47			39.10			33.92		
	38.68			37.91			36.91			38.49		
10 ¹ HAD ₅₀	39.11			38.41			38.39			35.34		
10 ⁰ HAD ₅₀												

HAD, virus isolation-erythrocyte adsorption assay; SD, standard deviation.

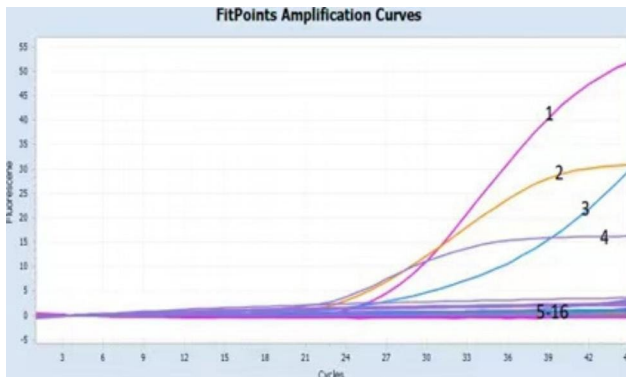


Fig. 3 Curves 1–4 represent *B646L*, *MGF505-3R*, *A137R*, and *EP402R* gene amplification profiles of African swine fever virus, respectively, and 5–16 represent pseudorabies virus, porcine parvovirus, porcine circovirus II, foot and mouth disease virus, classical swine fever virus, porcine epidemic diarrhea virus, transmissible gastroenteritis virus, swine influenza virus, Japanese encephalitis virus, porcine reproductive and respiratory syndrome virus, bovine viral diarrhea virus, and negative control, respectively

The *B646L*, *EP402R*, and *A137R* primers/probes used in this study were conserved in genotypes I and II ASFV. In addition, the *MGF505-3R* primers/probes were conserved in genotype I Benin 97/1 (AM712239), L60 (KM262844), and genotype II ASFV. However, deletions were found in OURT 88/3 (NC_044957) and in the frequently isolated Chinese genotypes HeN/ZZ-P1/2021 (MZ945536) and SD/DY-I/2021 (MZ945537). With this method, we inferred that a sample with positive results for *B646L*, *EP402R*, and *A137R* and negative results for *MGF505-3R* could contain genotype I ASFV. Moreover, we verified this result with a known genotype I ASFV cytotoxic sample (see Fig. 4E), and the results were consistent with our hypothesis.

To verify the specificity of the method, we performed amplification using nucleic acids of three porcine-derived DNA viruses (PRV, PPV, and PCVII) and eight porcine-derived RNA viruses (FMDV, CSFV, PEDV, TGEV, SIV,

JEV, PRRSV, and BVDV). None of these 11 nucleic acids showed amplification curves; only the positive ASFV control showed typical amplification (see Fig. 3), indicating that the method was specific for diagnosing ASFV without interference from other pathogens. Regarding reproducibility, the coefficient of variation was calculated for triplicate determination within each group, and the results obtained for all four genes were <2% less than that of other ASFV qPCR diagnostic methods [32]. This result indicated that our method was reproducible, with minimal deviation in the results obtained from each experiment, and that batch differences do not affect the determination of the results.

Regarding sensitivity, the minimum limit of detection for all four genes was 50 copies/μL and 10² HAD₅₀/mL. Moreover, our method was more sensitive for the detection of *B646L* and *EP402R* than other qPCR methods [33]. Because of the interference of the fluorescent groups in each probe of the quadruple qPCR, the hydrolysis efficiency of the probes was affected, changing the amplification efficiency. However, these effects were within a reasonable range, and the determination of negative results was unaffected. In addition, the method allowed the simultaneous detection of four genes, shortening the time of multigene detection.

A limitation of our study is that only four genes could be detected as only a maximum of four fluorescence channels are available in the current fluorescence PCR instruments. In the future these instruments may improve to include more fluorescence channels, which would allow for detection of additional genes.

In conclusion, we established a quadruple qPCR method for *B646L*, *EP402R*, *A137R*, and *MGF505-3R* to distinguish ASFV wild-type strains from gene-deleted strains based on current research. This method is the only qPCR method that can simultaneously detect four ASFV genes with conserved primer/probe sequences

Table 5 Intra-group reproducibility of the quadruple quantitative polymerase chain reaction groups

Target gene	Concentration (copies/μL)	Intra-group replication			Repeated between groups		
		Mean	SD	CV%	Mean	SD	CV%
<i>B646L</i>	1 × 10 ⁶	21.70	0.05	0.2	21.93	0.21	1
	1 × 10 ⁵	24.92	0.03	0.1	25.15	0.2	0.8
	1 × 10 ⁴	29.23	0.06	0.2	29.76	0.47	1.6
<i>EP402R</i>	1 × 10 ⁶	21.23	0.03	0.1	21.43	0.21	1
	1 × 10 ⁵	24.62	0.06	0.2	24.77	0.19	0.8
	1 × 10 ⁴	28.97	0.22	0.8	29.40	0.38	1.3
<i>A137R</i>	1 × 10 ⁶	20.97	0.03	0.1	21.24	0.24	1.1
	1 × 10 ⁵	24.56	0.13	0.5	24.74	0.20	0.8
	1 × 10 ⁴	29.14	0.23	0.8	29.62	0.42	1.4
<i>MGF505-3R</i>	1 × 10 ⁶	17.97	0.02	0.1	18.31	0.32	1.7
	1 × 10 ⁵	21.86	0.11	0.5	22.26	0.37	1.7
	1 × 10 ⁴	26.94	0.20	0.7	27.50	0.52	1.9

SD, standard deviation; CV, coefficient of variation.

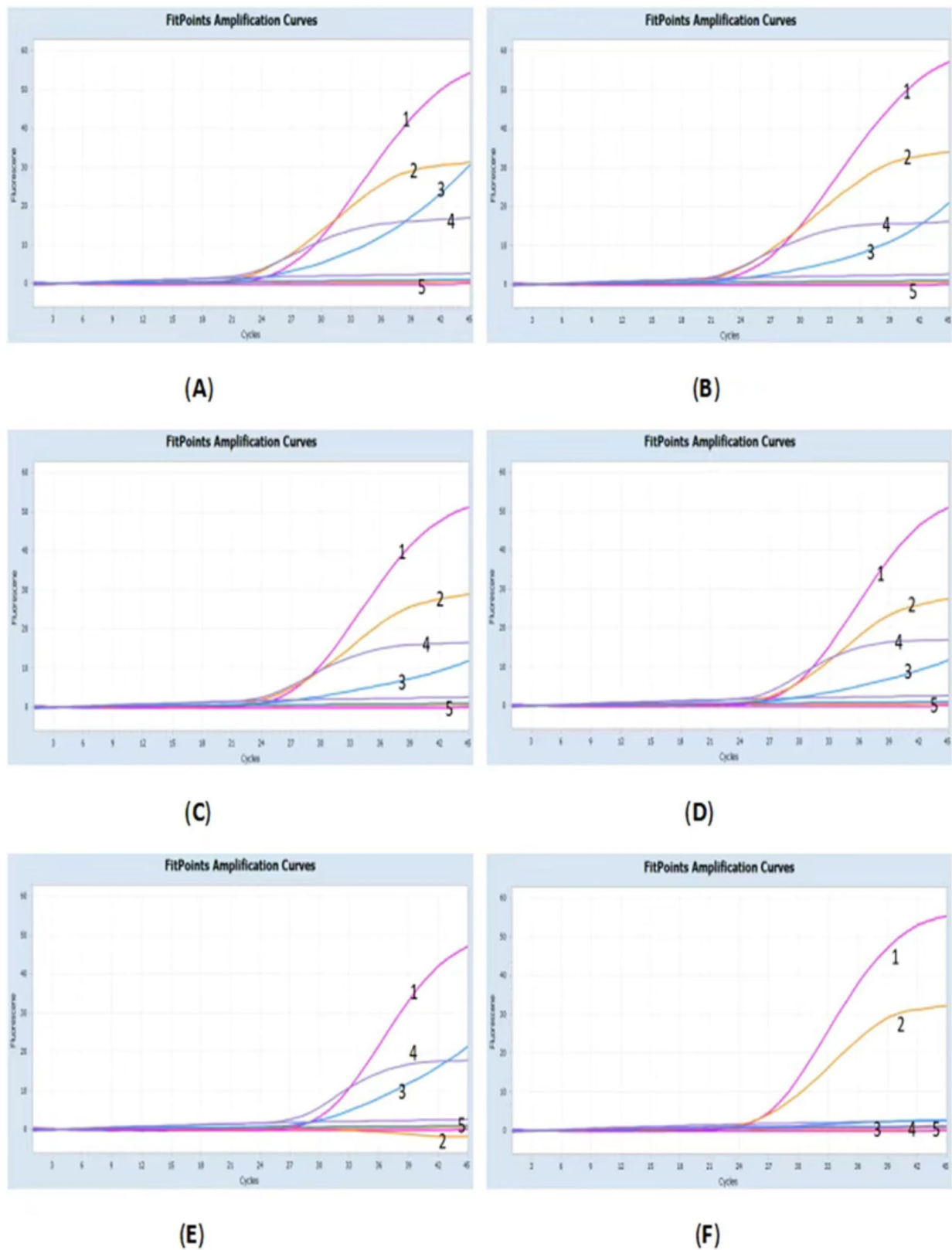


Fig. 4 Amplification curves for (A) the genotype II African swine fever virus (ASFV) blood sample, (B) the genotype II ASFV liver sample, (C) the genotype II ASFV spleen sample, (D) the genotype II ASFV lung sample, (E) the genotype I cell sample, and (F) the ASFV Δ A137R Δ EP402R cell sample. Numbers 1–5 indicate ASFV *B646L*, *MGF505-3R*, *A137R*, *ER402R*, and negative control amplification curves, respectively

with high sensitivity, specificity, and reproducibility, providing a comprehensive diagnosis of ASFV.

Abbreviations

ASF	African swine fever
ASFV	African swine fever virus
BVDV	Bovine viral diarrhoea virus
CSFV	Classical swine fever virus
FMDV	Foot and mouth disease virus
HAD	Virus isolation–erythrocyte adsorption assay
JEV	Japanese encephalitis virus
MGF	Multigene family
PCVII	Porcine epidemic diarrhoea virus
PEDV	Porcine epidemic diarrhoea virus
PPV	Porcine parvovirus
PRRSV	Porcine reproductive and respiratory syndrome virus
PRV	Pseudorabies virus
qPCR	Quantitative polymerase chain reaction
SIV	Swine influenza virus
TGEV	Transmissible gastroenteritis virus

Supplementary Information

The online version contains supplementary material available at <https://doi.org/10.1186/s12985-023-02111-1>.

Supplementary Material 1

Supplementary Material 2

Supplementary Material 3

Acknowledgements

We thank Shanxi Agricultural University and the Biosafety Level III Laboratory of China Veterinary Drug Inspection Institute for their support towards the completion of this study.

Author contributions

ZXQ, XYJ, and ZQZ designed the experimental protocol. ZXZ and PGR completed the experiment. ZXZ wrote and submitted the manuscript. WC, XL, ZYY, LYB, and ZJJ assisted in the experiment and provided guidance. ZXQ and WHD revised the manuscript. All authors read and approved the final version of the submitted manuscript.

Funding

This work was funded by the National Key Research and Development Program of China (2021YFD1800105-1), the “SixNew” Project of Agriculture and Rural Department of Shanxi Province, and the Fund for Shanxi “1331Project” Key Innovative Research Team (No. 20211331-16).

Author Contributions

ZXQ, XYJ, and ZQZ designed the experimental protocol. ZXZ and PGR completed the experiment. ZXZ wrote and submitted the manuscript. WC, XL, ZYY, LYB, and ZJJ assisted in the experiment and provided guidance. ZXQ and WHD revised the manuscript. All authors read and approved the final version of the submitted manuscript.

Data Availability

All data generated or analysed during this study are included in this published article and its supplementary information files.

Declarations

Ethics approval and consent to participate

Not applicable.

Consent for publication

Not applicable.

Competing interests

The authors declare that they have no competing interests.

Received: 10 May 2023 / Accepted: 30 June 2023

Published online: 14 July 2023

References

- Bastos ADS, Penrith M-L, Crucière C, Edrich JL, Hutchings G, Roger F, et al. Genotyping field strains of african swine fever virus by partial p72 gene characterisation. *Arch Virol*. 2003;148:693–706. <https://doi.org/10.1007/s00705-002-0946-8>.
- Quembo CJ, Jori F, Vosloo W, Heath L. Genetic characterization of african swine fever virus isolates from soft ticks at the wildlife/domestic interface in Mozambique and identification of a novel genotype. *Transbound Emerg Dis*. 2017;1–12. <https://doi.org/10.1111/tbed.12700>.
- Alejo A, Matamoros T, Guerra M, Andrés G. A proteomic atlas of the African swine fever virus particle. *J Virol*. 2018;92:e01293-18. doi:10.1128/JVI.01293-18.
- Liu S, Luo Y, Wang Y, Li S, Zhao Z, Bi Y, et al. Cryo-EM structure of the African swine fever virus. *Cell Host & Microbe*. 2019;26:1–8. doi:10.1016/j.chom.2019.11.004.
- Zhao D, Liu R, Zhang X, Li F, Wang J, Zhang J, et al. Replication and virulence in pigs of the first african swine fever virus isolated in China. *Emerg Microbes Infect*. 2019;8:438–47. <https://doi.org/10.1080/22221751.2019.1590128>.
- Sun E, Huang L, Zhang X, Zhang J, Shen D, Zhang Z, et al. Genotype I african swine fever viruses emerged in domestic pigs in China and caused chronic infection. *Emerg Microbes Infect*. 2021;10:2183–93. <https://doi.org/10.1080/22221751.2021.1999779>.
- Borca MV, Kutish GF, Alfonso CL, Itusta P, Carrillo C, Brun A, et al. An african swine fever virus gene with similarity to the T-lymphocyte surface antigen CD2 mediates hemadsorption. *Virology*. 1994;199:463–8. <https://doi.org/10.1006/viro.1994.1146>.
- Chaulagain S, Delhon GA, Khatiwada S, Rock DL. African swine fever virus CD2v protein induces β -interferon expression and apoptosis in swine peripheral blood mononuclear cells. *Viruses*. 2021;13:1480. <https://doi.org/10.3390/v13081480>.
- Chapman DAG, Tcherepanov V, Upton C, Dixon LK. Comparison of the genome sequences of non- pathogenic and pathogenic African swine fever virus isolates. *J Gen Virol*. 2008;89:397–408. doi:10.1099/vir.0.83343-0.
- Ramirez-Medina E, Vuono E, Silva E, Rai A, Valladares A, Pruitt S, et al. Evaluation of the deletion of MGF110-5L-6L on swine virulence from the pandemic strain of african swine fever virus and use as a DIVA marker in vaccine candidate ASFV-G- Δ 1177L. *J Virol*. 2022;96:e00597–22. <https://doi.org/10.1128/jvi.00597-22>.
- Zhu Z, Chen H, Liu L, Cao Y, Jiang T, Zou Y, et al. Classification and characterization of multigene family proteins of african swine fever viruses. *Brief Bioinform*. 2021;22:bbaa380. <https://doi.org/10.1093/bib/bbaa380>.
- Sun M, Yu S, Ge H, Wang T, Li Y, Zhou P, et al. The A137R protein of african swine fever virus inhibits type I interferon production via the autophagy-mediated lysosomal degradation of TBK1. *J Virol*. 2022;96:e0195721. <https://doi.org/10.1128/jvi.01957-21>.
- Gallardo C, Soler A, Rodze I, Nieto R, Cano-Gómez C, Fernandez-Pinero J, Arias M. Attenuated and non-haemadsorbing (non-HAD) genotype II African swine fever virus (ASFV) isolated in Europe, Latvia 2017. *Transbound Emerg Dis*. 2019;66:1399 – 404. doi:10.1111/tbed.13132.
- Belák A, Thorén P. Molecular diagnosis of animal diseases: some experiences over the past decade. *Expert Rev Mol Diagn*. 2002;1(4):434–43. <https://doi.org/10.1586/14737159.1.4.434>.
- Qiu Z, Li Z, Yan Q, Li Y, Xiong W, Wu K, et al. Development of diagnostic tests provides technical support for the control of african swine fever. *Vaccines*. 2021;9:343. <https://doi.org/10.3390/vaccines9040343>.
- Ward MP, Tian K, Nowotny N. African swine fever, the forgotten pandemic. *Transbound Emerg Dis*. 2021;68:2637–9.
- Wu K, Liu J, Wang L, Fan S, Li Z, Li Y, et al. Current state of global african swine fever vaccine development under the prevalence and transmission of ASF in China. *Vaccines*. 2020;8:531. <https://doi.org/10.3390/vaccines8030531>.
- Caixia W, Songyin Q, Ying X, Haoyang Y, Haoxuan L, Shaoqiang W, et al. Development of a blocking ELISA kit for detection of ASFV antibody based on a monoclonal antibody against full-length p72. *J AOAC Int*. 2022;105:1428–36. <https://doi.org/10.1093/jaoacint/qsac050>.
- Geng R, Sun Y, Li R, Yang J, Ma H, Qiao Z, et al. Development of a p72 trimer-based colloidal gold strip for detection of antibodies against african

- swine fever virus. *Appl Microbiol Biotechnol*. 2022;106:2703–14. <https://doi.org/10.1007/s00253-022-11851-z>.
20. Wang Y, Xu L, Noll L, Stoy C, Porter E, Fu J, et al. Development of a real-time PCR assay for detection of african swine fever virus with an endogenous internal control. *Transbound Emerg Dis*. 2020;67:2446–54. <https://doi.org/10.1111/tbed.13582>.
 21. Zhu W, Meng K, Zhang Y, Bu Z, Zhao D, Meng G. Lateral flow assay for the detection of african swine fever virus antibodies using gold nanoparticle-labeled acid-treated p72. *Front Chem*. 2021;9:804981. <https://doi.org/10.3389/fchem.2021.804981>.
 22. Lv C, Zhao Y, Jiang L, Zhao L, Wu C, Hui X, et al. Development of a dual ELISA for the detection of CD2v-unexpressed lower-virulence mutational ASFV. *Life*. 2021;11:1214. <https://doi.org/10.3390/life11111214>.
 23. Niu Y, Zhang G, Zhou J, Liu H, Chen Y, Ding P, et al. Differential diagnosis of the infection caused by wild-type or CD2v-deleted ASFV strains by quantum dots-based immunochromatographic assay. *Lett Appl Microbiol*. 2022;74:1001–7. <https://doi.org/10.1111/lam.13691>.
 24. Hemmink JD, Khazalwa EM, Abkallo HM, Oduor B, Khayumbi J, Svitek N, et al. Deletion of the CD2v gene from the genome of ASFV-Kenya-IX-1033 partially reduces virulence and induces protection in pigs. *Viruses*. 2022;14:1917. <https://doi.org/10.3390/v14091917>.
 25. Pérez-Núñez D, Sunwoo SY, García-Belmonte R, Kim C, Vigara-Astillero G, Riera E, et al. Recombinant african swine fever virus Arm/07/CBM/c2 lacking CD2v and A238L is attenuated and protects pigs against virulent korean Paju strain. *Vaccines*. 2022;10:1992. <https://doi.org/10.3390/vaccines10121992>.
 26. Koltsova G, Koltsov A, Krutko S, Kholod N, Tulman ER, Kolbasov D. Growth kinetics and protective efficacy of attenuated ASFV strain Congo with deletion of the EP402 gene. *Viruses*. 2021;13:1259. <https://doi.org/10.3390/v13071259>.
 27. Fan Y, Chen W, Jiang C, Zhang X, Sun Y, Liu R et al. Host responses to live-attenuated ASFV (HLJ/18-7GD). *Viruses*. 2022;14: 2003. <https://doi.org/10.3390/v14092003>.
 28. Li D, Liu Y, Qi X, Wen Y, Li P, Ma Z, et al. African swine fever virus MGF-110-9L-deficient mutant has attenuated virulence in pigs. *Virology*. 2021;36:187–95. <https://doi.org/10.1007/s12250-021-00350-6>.
 29. Bourry O, Hutet E, Le Dimna M, Lucas P, Blanchard Y, Chastagner A, et al. Oronasal or intramuscular immunization with a thermo-attenuated ASFV strain provides full clinical protection against Georgia 2007/1 challenge. *Viruses*. 2022;14:2777. <https://doi.org/10.3390/v14122777>.
 30. Gladue DP, Ramirez-Medina E, Vuono E, Silva E, Rai A, Pruitt S, et al. Deletion of the A137R gene from the pandemic strain of african swine fever virus attenuates the strain and offers protection against the virulent pandemic virus. *J Virol*. 2021;95:e0113921. <https://doi.org/10.1128/jvi.01139-21>.
 31. Sun E, Zhang Z, Wang Z, He X, Zhang X, Wang L, et al. Emergence and prevalence of naturally occurring lower virulent african swine fever viruses in domestic pigs in China in 2020. *Sci China Life Sci*. 2021;64:752–65. <https://doi.org/10.1007/s11427-021-1904-4>.
 32. Yang H, Peng Z, Song W, Zhang C, Fan J, Chen H, et al. A triplex real-time PCR method to detect african swine fever virus gene-deleted and wild type strains. *Front Vet Sci*. 2022;9:943099. <https://doi.org/10.3389/fvets.2022.943099>.
 33. Cao S, Lu H, Wu Z, Zhu S. A duplex fluorescent quantitative PCR assay to distinguish the genotype I and II strains of african swine fever virus in chinese epidemic strains. *Front Vet Sci*. 2022;9:998874. <https://doi.org/10.3389/fvets.2022.998874>.

Publisher's Note

Springer Nature remains neutral with regard to jurisdictional claims in published maps and institutional affiliations.